Probing the electroweak sector with single- and multiboson measurements at the LHC

Elementary Particle Physics Seminar, Warwick

The
University
Of
Sheffield.

Philip Sommer

University of Sheffield

28.10.2021

The Standard Model

- The Standard Model describes the fundamental constituents of matter and their interactions
  - strong and electroweak (EW) interaction
- Rich variety of interactions derived from a rather simple set of symmetries
- Self-interactions of electroweak gauge bosons
  - Quantum corrections at EW mass scale (probed in W/Z precision measurements)
  - Large effects at highest energies
- At the LHC we can test the electroweak theory at highest energies

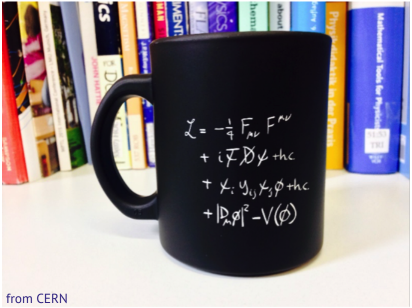

from CERN

$\mathrm{SU}(3)_C$ ×	$\mathrm{SU}(2)_L$ ×	$\mathrm{U}(1)_Y$
colour red, green, blue	weak isospin $I_3 = 0, \pm\frac{1}{2}$	weak hypercharge Y
8 gluons	W^1, W^2, W^3	B
	$\to W^+, W^-, Z, \gamma$	

Electroweak Theory

- Gauge couplings arise from the SU(2) potential term $\mathcal{L} = -\frac{1}{4} W^a_{\mu\nu} W^{\mu\nu}_a$, with the field strength tensor $W^a_{\mu\nu} = \partial_\mu W^a_\nu - \partial_\nu W^a_\mu - g f_{abc} W^b_\mu W^c_\nu$
- It generates cubic and quartic couplings

$$
\begin{aligned}
\mathcal{L}_3 &= i e_{V=\gamma,Z} \left[W^+_{\mu\nu} W^{-\mu} V^\nu - W^-_{\mu\nu} W^{+\mu} V^\nu + W^+_\mu W^-_\nu V^{\mu\nu} \right] \\
\mathcal{L}_4 &= e^2_W \quad \left[W^-_\mu W^{+\mu} W^-_\nu W^{+\nu} - W^-_\mu W^{-\mu} W^+_\nu W^{+\nu} \right] \\
&\quad + e^2_{V=\gamma,Z} \left[W^-_\mu W^{+\mu} V_\nu V^\nu - W^-_\mu V^\mu W^+_\nu Z^\nu \right] \\
&\quad + e_\gamma e_Z \left[2 W^-_\mu W^{+\mu} Z_\nu A^\nu - W^-_\mu Z^\mu W^+_\nu A^\nu - W^-_\mu A^\mu W^+_\nu Z^\nu \right]
\end{aligned}
$$

- With precise predictions of the coupling strength:

$e_\gamma = g \sin\theta_W$, $e_W = \dfrac{e_\gamma}{2\sqrt{2}\sin\theta_W}$ and $e_Z = e_\gamma \cot\theta_W$

- They *always* involve a pair of W bosons, there are no neutral vertices
- Heavy gauge bosons also couple to the Higgs boson

$$\mathcal{L}_{\text{Higgs}} = \frac{m^2_W}{v^2} W^+_\mu W^{-\mu} h^2 + \frac{m^2_Z}{v^2} Z_\mu Z^\mu h^2$$

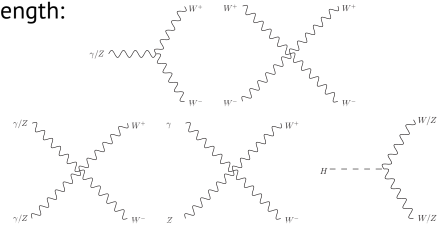

Gauge Cancellations

- Gauge-boson self interactions play a crucial role for the renormalisability of the electroweak theory
- Large cancellations of divergences arising in individual diagrams are exact if couplings take the values of the SM

→ Diboson measurements are a sensitive probe of the inner structure of the electroweak symmetry

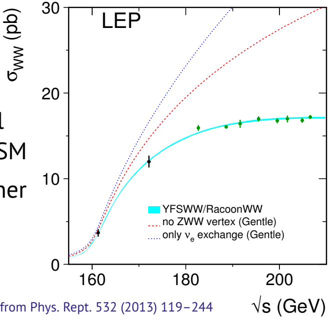

from Phys. Rept. 532 (2013) 119–244

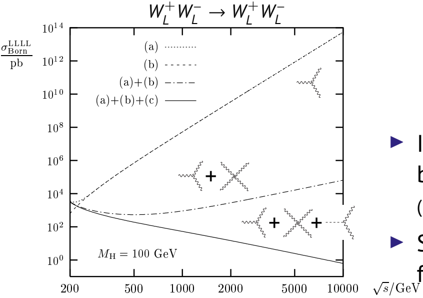

from Nucl. Phys. B525 (1998) 27-50

- In processes involving quartic couplings, the Higgs boson is governing the high-energy behaviour
  (if only massive gauge bosons participate in the scattering)
- Such processes became experimentally accessible for first time in the LHC run-2

Experimental Probes

Trilinear Self-interactions

- Diboson production

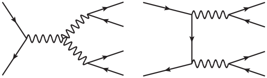

- Electroweak single-boson production

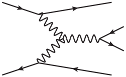

Quartic Self-interactions

- Triboson production

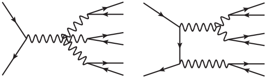

- Electroweak diboson production

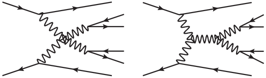

- Any process involving quartic self-interactions

- Showing today:
  - electroweak *Zjj* production
  - EFT interpretation of *VV* meas.

- Showing today:
  - electroweak $Z\gamma jj$ production
  - *WWW* production

Vector-boson Fusion (VBF)
and Vector-boson Scattering (VBS)

Vector-boson Fusion and Vector-boson Scattering

- Quartic *electroweak* (EW) coupling experimentally accessible in EW production of *VVjj*
- Electroweak production of *Vjj* sensitive to trilinear EW couplings

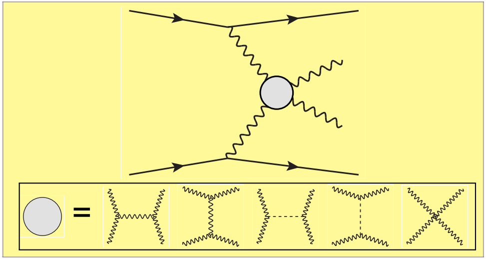

Purely electroweak interactions involving only cubic and quartic self interactions 🟡

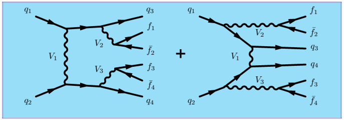

Purely electroweak interactions without self interactions 🔵

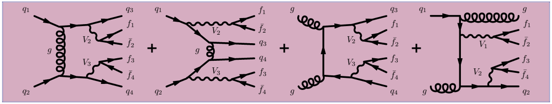

Processes involving both strong and electroweak interactions 🟣

🟡+🔵 not gauge-invariantly separable → measure EW production

(🟡/🔵)+🟣 interference, subtracted from data or a modelling uncertainty

Experimental Signature

- No colour connection between scattering quarks leads to characteristic signature

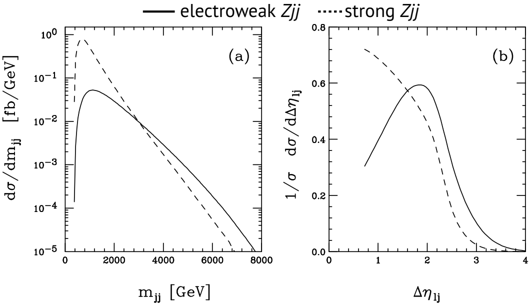

PRD 54 (1996) 6680-6689

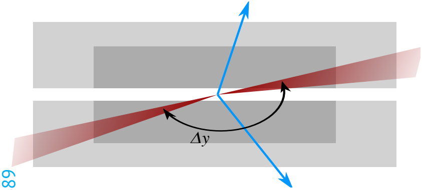

- Additional activity in the event measured relative to centre of “tagging jets”, e.g.:

$$\zeta_X = \left| \frac{y_X - \left(y_{j1} + y_{j2}\right)/2}{y_{j1} - y_{j2}} \right|, \qquad C_X = \exp\left[-4 \left(\frac{\eta_X - \left(\eta_{j1} + \eta_{j2}\right)/2}{\eta_{j1} - \eta_{j2}} \right)^2 \right]$$

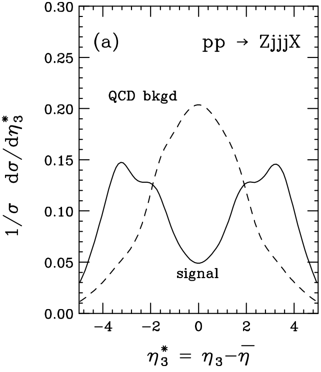

Phys. Rev. D 54 (1996) 6680-6689

Electroweak *Zjj* Production

EPJC 81 (2021) 163

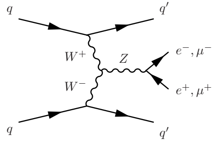

- Electroweak *Zjj* production as standard candle to benchmark theoretical calculations of VBF/VBS
- Critical for precise measurements of *Zjj*-electroweak is a good understanding of *Zjj*-strong background

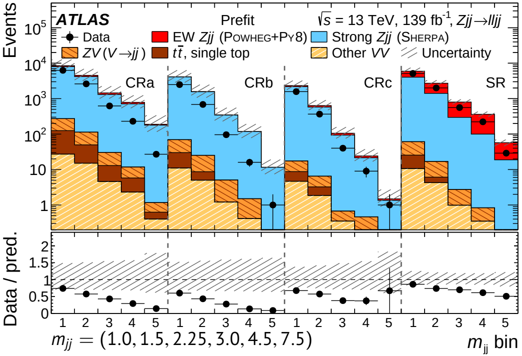

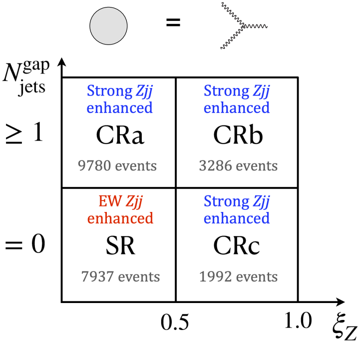

$N^{\text{gap}}_{\text{jets}}$ ≥ 1	Strong *Zjj* enhanced CRa 9780 events	Strong *Zjj* enhanced CRb 3286 events
$= 0$	EW *Zjj* enhanced SR 7937 events	Strong *Zjj* enhanced CRc 1992 events
	0.5	1.0 ξ_Z

- Strong *Zjj* estimation relies on *Z* centrality and central jet activity

Electroweak *Zjj* Results

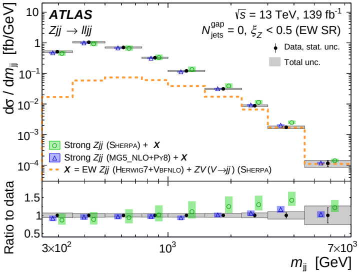

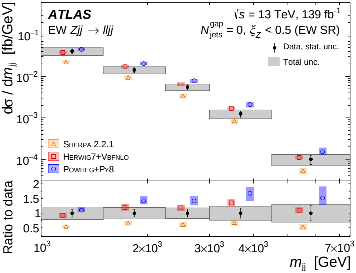

- Inclusive *Zjj* cross sections measured in signal and EW-suppressed phase space + *Zjj*-electroweak cross section in SR (m_{jj}, $p_{\mathrm{T}}(ll)$, Δy_{jj}, $\Delta\phi_{jj}$)
- Dominant uncertainty in *Zjj*-strong modelling and jet-energy scale and resolution
- Powerful EFT interpretation, including CP sensitive operators

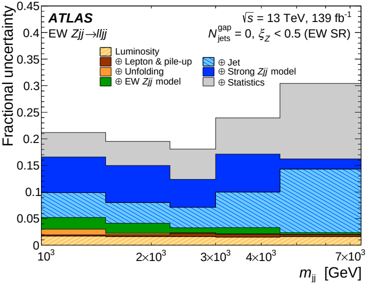

Electroweak $Z(\rightarrow \ell\ell)\gamma jj$ Production

ATLAS-CONF-2021-038

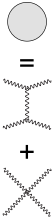

Lepton	$p_{\mathrm{T}}^{\ell} > 20, 30(\text{leading})$ GeV, $\lvert\eta_\ell\rvert < 2.47$ $N_\ell \geq 2$
Photon	$E_{\mathrm{T}}^{\gamma} > 25$ GeV, $\lvert\eta_\gamma\rvert < 2.37$ $E_{\mathrm{T}}^{cone20} < 0.07 E_{\mathrm{T}}^{\gamma}$ $\Delta R(\ell,\gamma) > 0.4$
Jet	$p_{\mathrm{T}}^{jet} > 50$ GeV, $\lvert y_{jet}\rvert < 4.4$ $\lvert\Delta y\rvert > 1.0$ $m_{jj} > 150$ GeV remove jets if $\Delta R(\gamma, j) < 0.4$ or if $\Delta R(\ell, j) < 0.3$
Event	$m_{\ell\ell} > 40$ GeV $m_{\ell\ell} + m_{\ell\ell\gamma} > 182$ GeV $\zeta(\ell\ell\gamma) < 0.4$ $N_{jets}^{gap} = 0$

VBS signatu

strong-$Z\gamma jj$ separation

(fiducial phase space selection)

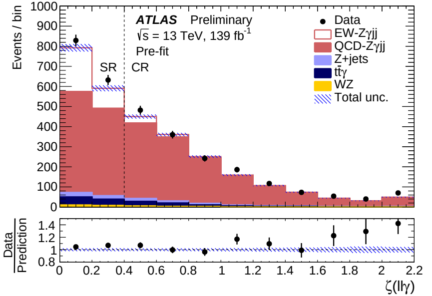

- Centrality used to control background from strong $Z\gamma jj$ (with a jet-veto for improved background modelli
- Background from misidentified photons estimated in data, background from $t\bar{t}\gamma$ validated in data

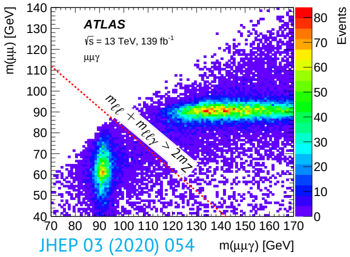

JHEP 03 (2020) 054

Electroweak $Z(\to \ell\ell)\gamma jj$ Analysis

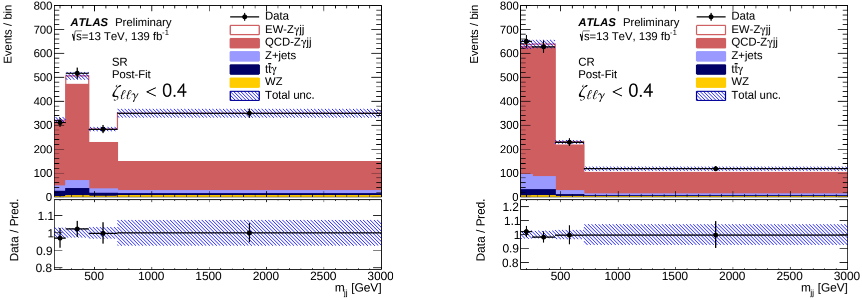

Sample	SR	CR
$N_{EW-Z\gamma jj}$	300 ± 36	55 ± 7
$N_{QCD-Z\gamma jj}$	987 ± 55	1352 ± 60
$N_{t\bar{t}\gamma}$	72 ± 11	59 ± 9
N_{WZ}	17 ± 3	14 ± 3
N_{Z+jets}	85 ± 30	143 ± 43
Total	1461 ± 38	1624 ± 40
N_{obs}	1461	1624

- To minimise dependence on theory modelling, the high-$\zeta_{\ell\ell\gamma}$ is only used to constrain the m_{jj} distribution
- Normalisation of strong $Z\gamma jj$ production is obtained separately in signal and control regions

$$\beta_{Z\gamma\text{-strong, CR}} = 1.00^{+0.18}_{-0.16}$$
$$\beta_{Z\gamma\text{-strong, SR}} = 1.06^{+0.17}_{-0.16}$$

Electroweak $Z(\rightarrow \ell\ell)\gamma jj$ Results

- Background-only hypothesis rejected with 10σ (exp. 11σ)
- Measured and theoretical $Z\gamma$-EW cross sections:

$$\sigma_{\text{EW, meas.}} = 4.49 \pm 0.40\ (\text{stat.}) \pm 0.42\ (\text{syst.})\ \text{fb}$$

$$\sigma_{\text{EW, theo.}} = 4.73 \pm 0.01\ (\text{stat.}) \pm 0.15\ (\text{PDF})^{+0.23}_{-0.22}\ (\text{scale})\ \text{fb}$$

(from `MG5_aMC@NLO+Pythia8` at LO)

- Measured and theoretical $Z\gamma$-EW+QCD cross sections:

$$\sigma_{\text{EW+QCD, meas.}} = 20.6 \pm 0.6\ (\text{stat.})^{+1.2}_{-1.0}\ (\text{syst.})\ \text{fb}$$

$$\sigma_{\text{EW+QCD, theo.}} = 20.4 \pm 0.1\ (\text{stat.}) \pm 0.2\ (\text{PDF})^{+2.6}_{-2.0}\ (\text{scale})\ \text{fb}$$

(from `MG5_aMC@NLO+Pythia8`)

Uncertainty in $\sigma_{\text{EW, meas.}}$

Source	Size [%]
Electron/photon calibration	± 0.3
Photon	± 0.3
Backgrounds	± 1.0
Electron	± 1.1
Flavour tagging	± 1.1
Muon	± 1.1
MC stat.	± 1.4
Pileup	± 2.6
Jets	± 4.7
QCD-$Z\gamma jj$ modelling	$^{+4.8}_{-4.3}$
EW-$Z\gamma jj$ modelling	$^{+5.7}_{-4.6}$
Data stat.	± 8.8
Total	$^{+13.4}_{-12.6}$

includes 2% interference

$Z(\rightarrow \nu\nu)\gamma jj$ Introduction

- In the past, $Z\rightarrow \nu\nu$ analyses yielded more stringent constraints on non-SM couplings
- Seen e.g. in search for non-SM ZZ couplings

	$ZZ\rightarrow 2\ell 2\nu$ JHEP 10 (2019) 127	$ZZ\rightarrow 4\ell$ Phys. Rev. D 97 (2018) 032005
f_4^γ $[\times 10^{-3}]$	$[-1.3, 1.3]$	$[-2.4, 2.4]$
f_4^Z $[\times 10^{-3}]$	$[-1.1, 1.1]$	$[-2.1, 2.1]$
f_5^γ $[\times 10^{-3}]$	$[-1.3, 1.3]$	$[-2.4, 2.4]$
f_5^Z $[\times 10^{-3}]$	$[-1.1, 1.1]$	$[-2.0, 2.0]$

Expected limits on $ZZ\gamma$ and ZZZ couplings

- Using the missing transverse momentum to trigger $Z(\rightarrow\nu\nu)\gamma$ events
- This usually doesn't impact sensitivity to BSM effects, as these are expected at high energy

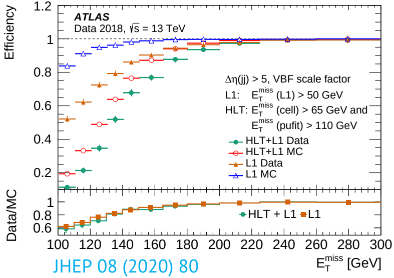

JHEP 08 (2020) 80

Electroweak $Z(\to \nu\nu)\gamma jj$ Production arXiv:2109.00925

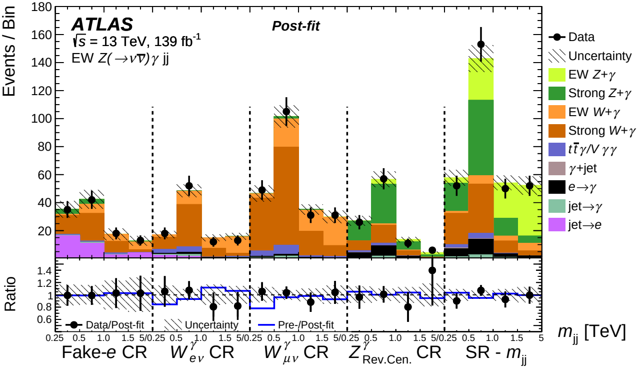

- Background-only hypothesis rejected with 5.2σ (exp. 5.1σ)
- Measured and theoretical $Z\gamma$-EW cross sections:

$$\sigma_{\text{EW, meas.}} = 1.31 \pm 0.20\ (\text{stat.}) \pm 0.20\ (\text{syst.})\ \text{fb}$$

$$\sigma_{\text{EW, theo.}} = 1.27 \pm 0.01\ (\text{stat.}) \pm 0.17\ (\text{scale}) \pm 0.03\ (\text{PDF})\ \text{fb}$$

(from `MG5_aMC@NLO+Pythia8` at LO, rescaled by 0.3% to `VBFNLO`)

- Largest sources of unc. in jet energy scale/reso. (7.6%) and $V\gamma$+jets modelling (6.7%)

Electroweak $W^{\pm}W^{\pm}jj$ and $WZjj$ Production

PRL 123 (2019) 161801
PLB 793 (2019) 469

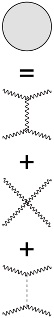

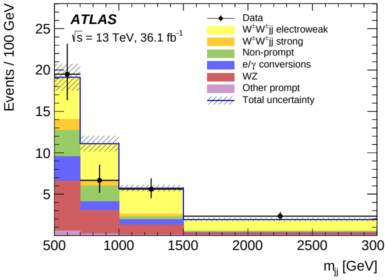

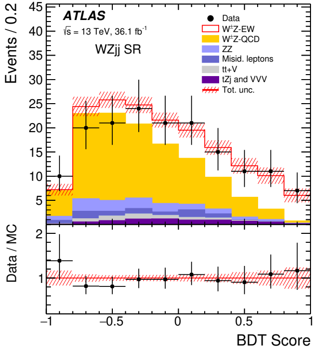

- The $W^{\pm}W^{\pm}jj$ and $WZjj$ channels have already been observed on a partial dataset of 36 fb
- They are theoretically understood well, at NLO EW⊗QCD (k-factors −10-15%)

- In the $W^{\pm}W^{\pm}jj$ final state, QCD and EW diagrams without self-interactions suppressed

⇒ Powerful tool for the study of electroweak symmetry breaking

Experimental Status

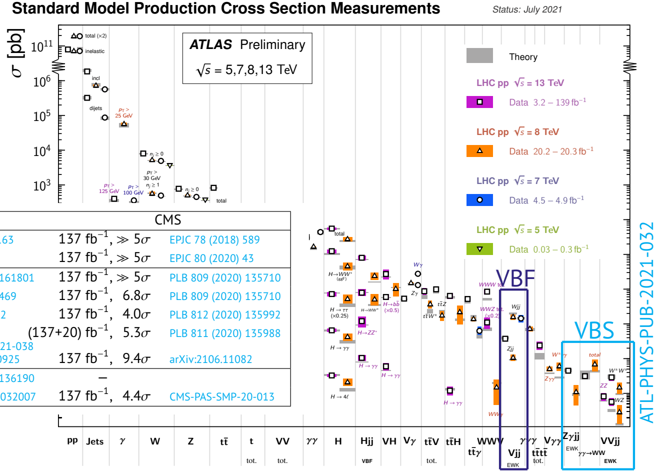

	ATLAS		CMS	
VBF Z	139 fb^{-1}, $\gg 5\sigma$	EPJC 81 (2021) 163	137 fb^{-1}, $\gg 5\sigma$	EPJC 78 (2018) 589
VBF W	–		137 fb^{-1}, $\gg 5\sigma$	EPJC 80 (2020) 43
VBS $W^\pm W^\pm$	36 fb^{-1}, 6.5σ	PRL 123 (2019) 161801	137 fb^{-1}, $\gg 5\sigma$	PLB 809 (2020) 135710
VBS $W^\pm Z$	36 fb^{-1}, 5.3σ	PLB 793 (2019) 469	137 fb^{-1}, 6.8σ	PLB 809 (2020) 135710
VBS ZZ	139 fb^{-1}, 5.5σ	arXiv:2004.10612	137 fb^{-1}, 4.0σ	PLB 812 (2020) 135992
VBS $W\gamma$	–		(137+20) fb^{-1}, 5.3σ	PLB 811 (2020) 135988
VBS $Z\gamma$	139 fb^{-1}, $> 10\sigma$	ATLAS-CONF-2021-038 arXiv:2109.00925	137 fb^{-1}, 9.4σ	arXiv:2106.11082
$\gamma\gamma \to W^+W^-$	139 fb^{-1}, 8.4σ	PLB 816 (2021) 136190	–	
VBS VV	36 fb^{-1}, 2.7σ	PRD 100 (2019) 032007	137 fb^{-1}, 4.4σ	CMS-PAS-SMP-20-013

- Electroweak *VVjj* production has been observed in all major channels in the LHC run-2
- They are amongst the rarest processes currently experimentally accessible

Triboson Production

Experimental Status

- Triboson production has been observed at 8 TeV in $Z\gamma\gamma$ (PRD 93 (2016) 112002) and $\gamma\gamma\gamma$ channels (PLB 781 (2018) 55 in agreement with the NNLO calculation in PLB 812 (2021) 136013)

- Evidence for *WVV* from ATLAS
  - in 80 fb^{-1} (2015-2017 data)
  - 4.1σ (*WVV*) and 3.2σ (*WWW*)
  - PLB 798 (2019) 134913

- Observation of *VVV* from CMS
  - in 137 fb^{-1} (2015-2018 data)
  - 5.7σ (*VVV*), 3.3σ (*WWW*)
  - PRL 125 (2020) 151802

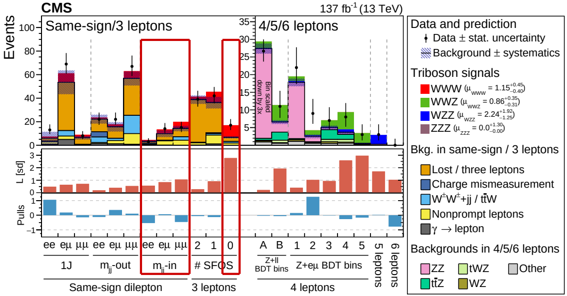

Phys. Rev. Lett. 125 (2020) 151802

New ATLAS result focusses on *WWW* in $\ell^{\pm}\nu\ell'^{\pm}\nu jj$ and $\ell^{\pm}\nu\ell'^{\mp}\nu\ell^{\pm}\nu$

- $e^{\pm}e^{\pm}$+2j, $e^{\pm}\mu^{\pm}$+2j, $\mu^{\pm}\mu^{\pm}$+2j (same-sign dilepton)
- $3\ell + E_{\mathrm{T}}^{\mathrm{miss}}$ with no same-flavour opposite-charge lepton pair

→ strong suppression of *VV*+jets

WWW Signal Definition

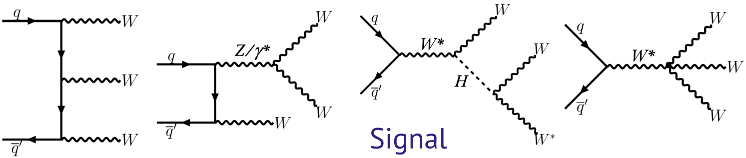

Signal

WWW Simulation

- on-shell *WWW* simulated with `Sherpa 2.2.2` at NLO
- $WH\rightarrow WWW^*$ simulated with `Powheg+Pythia8` at NLO
- spin correlations accounted for in *W* decays
- *t*- and *u*-channel production at $\mathcal{O}(\alpha^6)$ classified as background

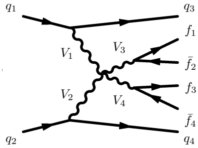

Background

WWW Analysis

- Experimentally, $WWW\rightarrow\ell^\pm\nu\ell^\pm\nu jj$ is distinguished from VBS signatures by requiring at least two central jets with $m_{jj} < 160$ GeV and $\left|\Delta\eta_{jj}\right| < 1.5$

Measurement in $\ell^\pm\ell^\pm 2j$ events

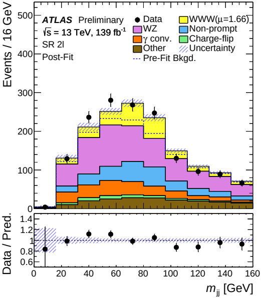

- Signal is measured in a fit to a BDT discriminant
- BDT modelling validated in control regions
  - the m_{jj} side bands
  - the *WZ* control region(s)
  - a *b*-tag control region

before unblinding signal region

2ℓ
$\lvert m_{jj} - m_W \rvert$
p_{T} (forward jet)
$E_{\mathrm{T}}^{\mathrm{miss}}$ significance
$p_T(j_2)$
minimum $m(\ell, j)$
$m(\ell_2, j_1)$
$N(\mathrm{jets})$
$p_{\mathrm{T}}\ (\ell_2)$
$m_{\ell\ell}$
$\lvert\eta(\ell_1)\rvert$
$N(\text{leptons in jets})$
$m(\ell_1, j_1)$

BDT training variables

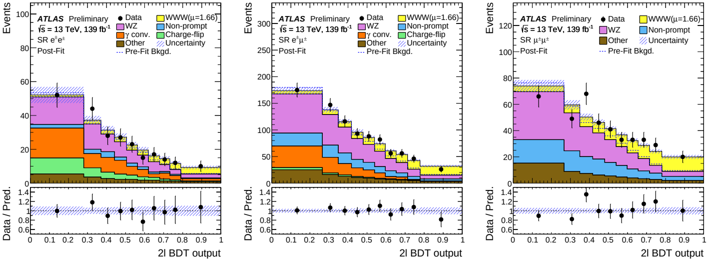

Measurement in 3ℓ events

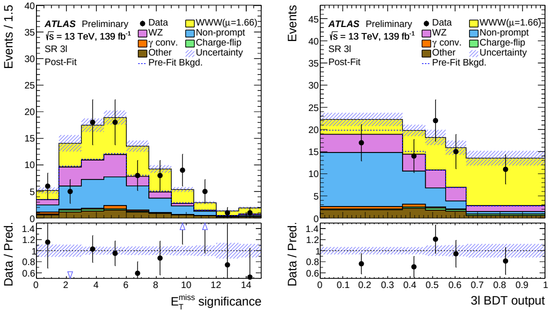

3ℓ
$E_{\mathrm{T}}^{\mathrm{miss}}$significance $\times 10/E_{\mathrm{T}}^{\mathrm{miss}}$
$p_T(\ell_2)$
N(jets)
same flavor $m_{\ell\ell}$
$m_T(\ell\ell\ell, E_{\mathrm{T}}^{\mathrm{miss}})$
$m(\ell_2, \ell_3)$
$\Delta\phi(\ell\ell\ell, E_{\mathrm{T}}^{\mathrm{miss}})$
minimum $\Delta R(\ell, \ell)$
$p_{\mathrm{T}}\ (\ell_3)$
$m_T(\ell_2, E_{\mathrm{T}}^{\mathrm{miss}})$
$E_{\mathrm{T}}^{\mathrm{miss}}$ significance

BDT training variables

- Higher signal purity in 3ℓ events compared to $\ell^\pm\ell^\pm jj$
- Separate BDT training to extract signal
- Kinematic and angular variables, combining leptons and $E_{\mathrm{T}}^{\mathrm{miss}}$
- Similar validation of BDT modelling as for $\ell^\pm\ell^\pm jj$

Backgrounds and Background Estimation

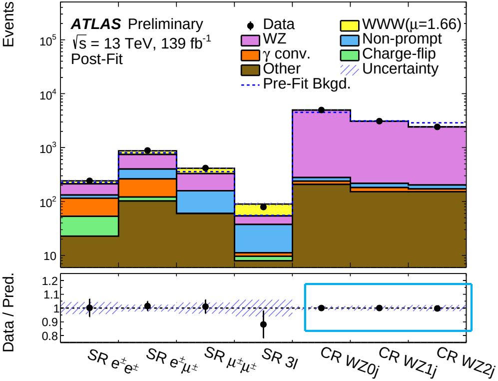

Normalization Factors		
$WZ + 0$ jets	$WZ + 1$ jet	$WZ + \geq 2$ jets
1.12 ± 0.11	0.98 ± 0.04	0.88 ± 0.18

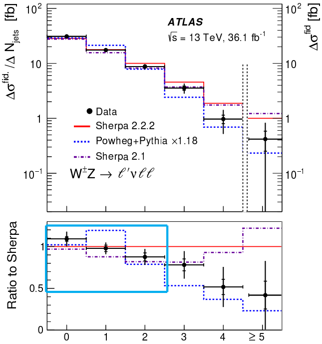

from Eur. Phys. J. C 79 (2019) 535

- Fit of BDT (SRs) and $m_{3\ell}$ (*WZ* CRs)
- Largest source of background from *WZ+jets* production, constrained in control regions
- Most other backgrounds are instrumental and estimated in data (misidentified leptons, photons conversions, electron charge misreconstruction)

Cross-section Measurement

- Background-only hypothesis rejected with 8.2σ, where 5.4σ are expected

Fit	Observed (expected) significances [σ]	$\mu(WWW)$
$e^{\pm}e^{\pm}$	2.3 (1.4)	1.69 ± 0.79
$e^{\pm}\mu^{\pm}$	4.6 (3.1)	1.57 ± 0.40
$\mu^{\pm}\mu^{\pm}$	5.6 (2.8)	2.13 ± 0.47
2ℓ	6.9 (4.1)	1.80 ± 0.33
3ℓ	4.8 (3.7)	1.33 ± 0.39
Combined	**8.2 (5.4)**	$\mathbf{1.66 \pm 0.28}$

(relative to NLO `Sherpa/Powheg+Pythia8` with $\sigma_{WWW} = 511 \pm 42$ fb)

Uncertainty source	$\Delta\sigma/\sigma$ [%]
Data-driven background	5.3
Prompt-lepton-background modeling	3.3
Jets and $E_{\mathrm{T}}^{\mathrm{miss}}$	2.8
MC statistics	2.8
Lepton	2.1
Luminosity	1.9
Signal modeling	1.5
Pile-up modeling	0.9
Total systematic uncertainty	9.5
Data statistics	11.2
WZ normalizations	3.3
Total statistical uncertainty	11.6

- The measured cross section, extrapolated to the total phase space, is:

$$\sigma_{WWW} = 850 \pm 100\ (\text{stat.}) \pm 80\ (\text{syst.})\ \text{fb}$$

- Compared to a theoretical calculation:

					δ^{EW} [%]	δ^{QCD} [%]
$W^-W^+W^+$	136^{+6}_{-5} (scale) ± 4 (PDF)	fb	JHEP 09 (2017) 034	NLO QCD + NLO EW	+6.6	+67.1
$W^+W^-W^-$	76^{+4}_{-3} (scale) ± 2 (PDF)	fb			+7.9	+71.2
$W^{\pm}H \rightarrow W^{\pm}W^+W^-$	293^{+1}_{-2} (scale) ${}^{+6}_{-5}$ (PDF) ± 3 (α_s)	fb	CERN-2013-004	NNLO QCD + NLO EW		
	505	fb				

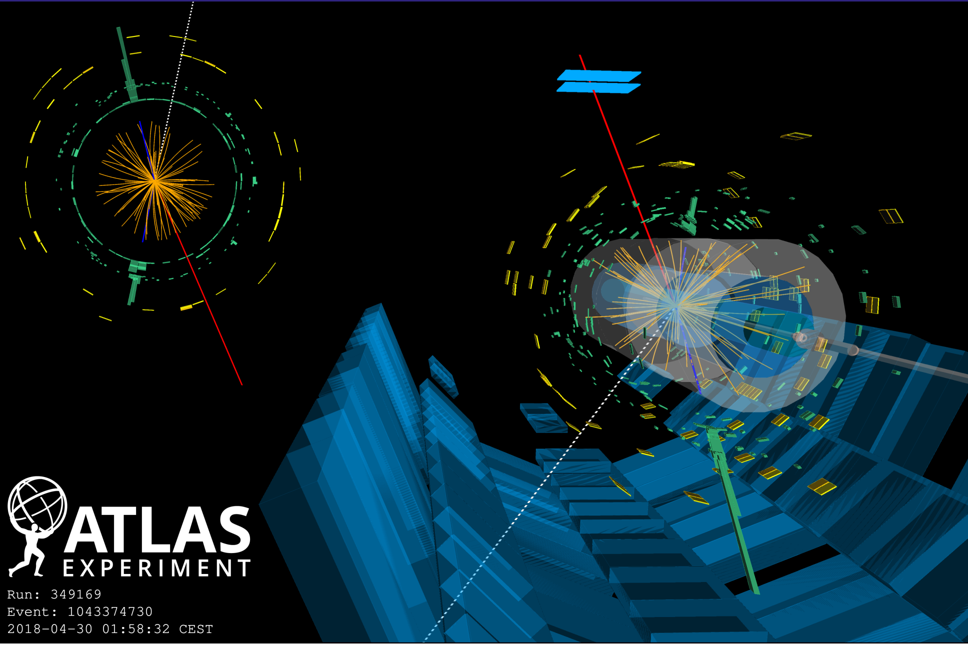

$WWW \to e^+ \nu e^+ \nu \mu^- \nu$ candidate event. The $E_{\mathrm{T}}^{\mathrm{miss}}$ has a magnitude of 105 GeV and the BDT score is 0.81.

Interpretation

The Standard Model Effective Field Theory

- Interpretation of multiboson measurements in the Standard Model Effective Theory (SMEFT)

→ Expansion of SM Lagrangian in increasing powers of inverse scale of new physics, $1/\Lambda$

$$\mathcal{L}_{\text{SMEFT}} = \mathcal{L}_{\text{SM}} + \sum_i \frac{c_i^{(6)}}{\Lambda^2}\mathcal{O}_i^{(6)} + \sum_i \frac{c_i^{(8)}}{\Lambda^4}\mathcal{O}_i^{(8)} + \ldots$$

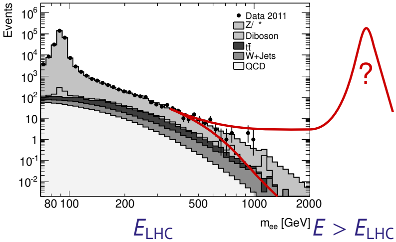

- Leading SMEFT effect expected from interference of dim-6 operators with SM:

$$\begin{aligned}\sigma &\sim |\mathcal{M}_{\text{SMEFT}}|^2 \\ &= |\mathcal{M}_{\text{SM}}|^2 + \underbrace{\underbrace{\sum_i \frac{c_i^{(6)}}{\Lambda^2} 2\text{Re}\left(\mathcal{M}_i^{(6)}\mathcal{M}_{\text{SM}}^*\right)}_{\textbf{linear model}} + \underbrace{\sum_i \frac{\left(c_i^{(6)}\right)^2}{\Lambda^4}\left|\mathcal{M}_i^{(6)}\right|^2}_{\text{quadratic terms}} + \underbrace{\sum_{i<j} \frac{c_i^{(6)}c_j^{(6)}}{\Lambda^4} 2\text{Re}\left(\mathcal{M}_i^{(6)}\mathcal{M}_j^{(6)*}\right)}_{\text{cross terms}}}_{\textbf{linear plus quadratic model}} + \ldots\end{aligned}$$

quadratic term at the same order, $\mathcal{O}\left(\Lambda^{-4}\right)$, as SM+dim-8 interference

- Focus on operators at dim-6
  - 33 CP-even operators studied, assuming flavour symmetry and neglecting Higgs

Experimental Input

- Combination of several multiboson measurements
  - $pp \to WW \to e\nu\mu\nu$: Eur. Phys. J. C 79 (2019) 884 using 36 fb^{-1}
  - $pp \to WZ \to \ell\ell\ell'\nu$: Eur. Phys. J. C 79 (2019) 535 using 36 fb^{-1}
  - $pp \to 4\ell \to \ell\ell\ell'\ell'$: JHEP 07 (2021) 005 using 139 fb^{-1}
  - $pp \to Zjj \to \ell\ell jj$: Eur. Phys. J. C 81 (2021) 163 using 139 fb^{-1}
- Measurements with high precision and small background contributions

  (assuming negligible effects of EFT on backgrounds)
- Sensitive to a large number of dim-6 operators affecting
  - gauge-boson self-couplings (though no neutral couplings at dim-6)
  - couplings of gauge bosons and fermions
  - four-fermion couplings

- Higgs-boson production kinematically suppressed:
  - see ATLAS-CONF-2020-053 for dedicated EFT study
  - see ATL-PHYS-PUB-2021-010 for a $H \to WW^*$ and WW combination

Kinematic Distributions

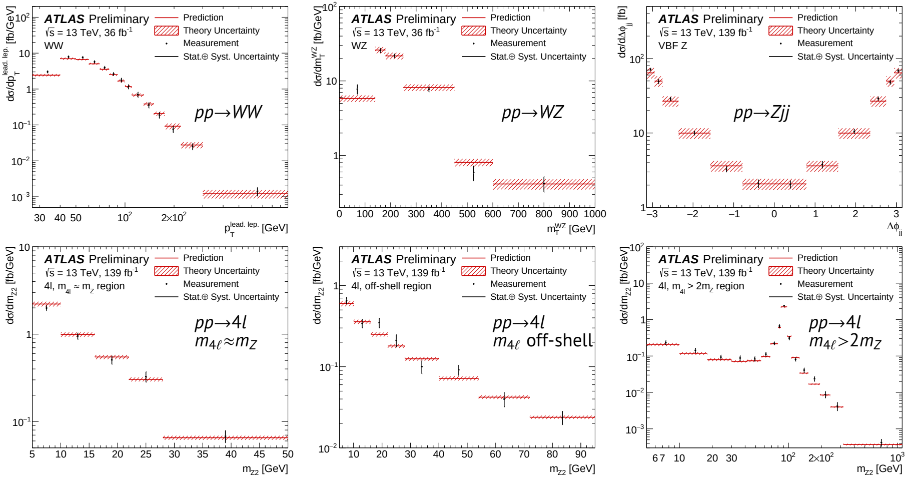

- Assuming smooth EFT effects have the folding matrix of the SM
  - Injection of BSM physics has been explicitly tested in $m_{4\ell}$ measurement

Experimental Sensitivity

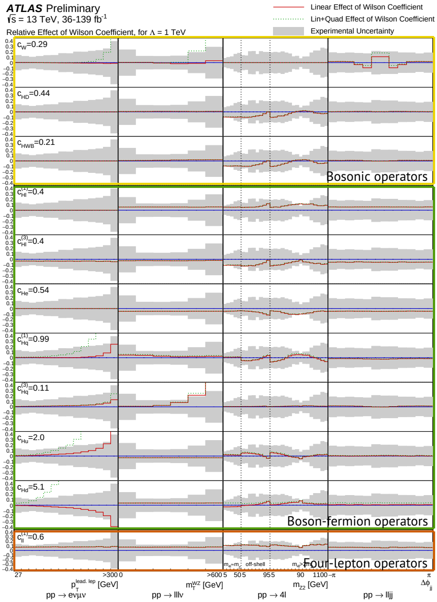

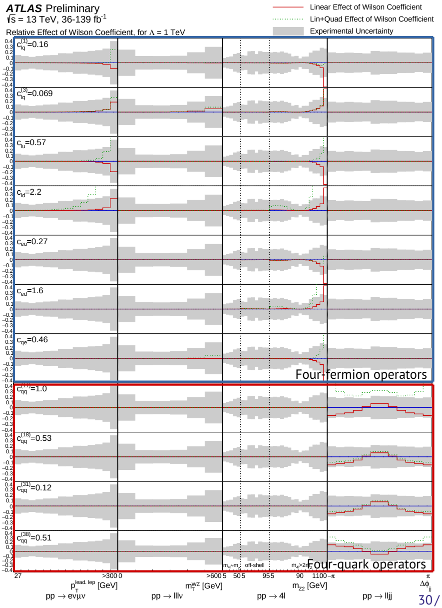

Experimental Sensitivity

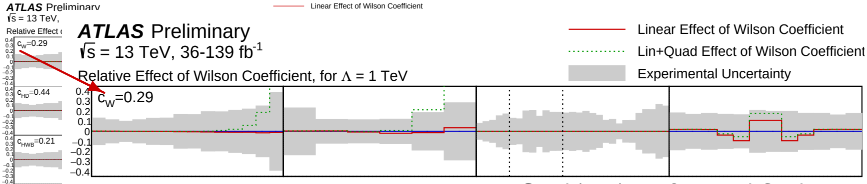

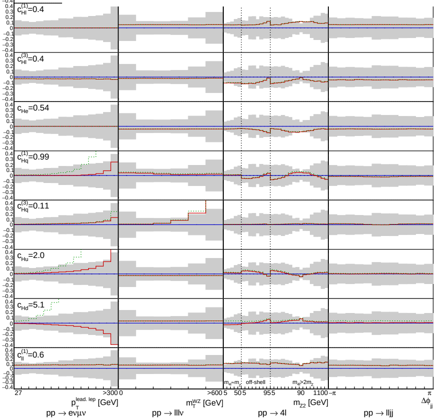

- Combination of several final states allows to improve limits

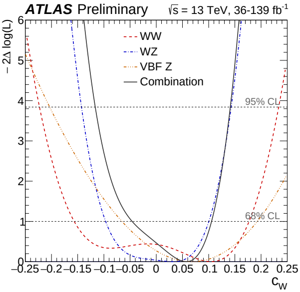

- Identified 33 sensitive CP-even coefficients in the Warsaw basis

Transformation of Basis

- Simultaneous constraints on multiple Wilson coefficients facilitated through complementarity of measurements

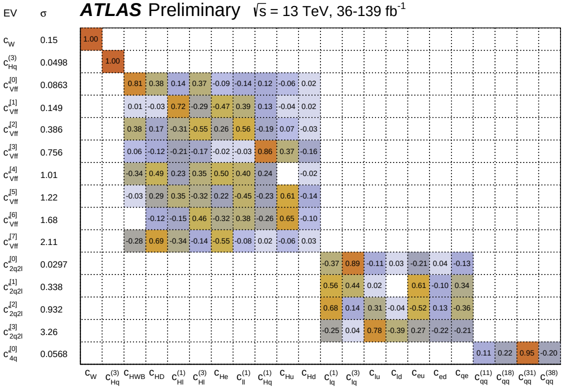

ATLAS Preliminary $\sqrt{s}$ = 13 TeV, 36-139 fb^{-1}

EV	σ	c_W	$c_{Hq}^{(3)}$	c_{HWB}	c_{HD}	$c_{Hl}^{(1)}$	$c_{Hl}^{(3)}$	c_{He}	$c_{ll}^{(1)}$	$c_{Hq}^{(1)}$	c_{Hu}	c_{Hd}	$c_{lq}^{(1)}$	$c_{lq}^{(3)}$	c_{lu}	c_{ld}	c_{eu}	c_{ed}	c_{qe}	$c_{qq}^{(11)}$	$c_{qq}^{(18)}$	$c_{qq}^{(31)}$	$c_{qq}^{(38)}$
c_W	0.15	1.00																					
$c_{Hq}^{(3)}$	0.0498		1.00																				
$c_{Vff}^{[0]}$	0.0863			0.81	0.38	0.14	0.37	-0.09	-0.14	0.12	-0.06	0.02											
$c_{Vff}^{[1]}$	0.149			0.01	-0.03	0.72	-0.29	-0.47	0.39	0.13	-0.04	0.02											
$c_{Vff}^{[2]}$	0.386			0.38	0.17	-0.31	-0.55	0.26	0.56	-0.19	0.07	-0.03											
$c_{Vff}^{[3]}$	0.756			0.06	-0.12	-0.21	-0.17	-0.02	-0.03	0.86	0.37	-0.16											
$c_{Vff}^{[4]}$	1.01			-0.34	0.49	0.23	0.35	0.50	0.40	0.24		-0.02											
$c_{Vff}^{[5]}$	1.22			-0.03	0.29	0.35	-0.32	0.22	-0.45	-0.23	0.61	-0.14											
$c_{Vff}^{[6]}$	1.68				-0.12	-0.15	0.46	-0.32	0.38	-0.26	0.65	-0.10											
$c_{Vff}^{[7]}$	2.11			-0.28	0.69	-0.34	-0.14	-0.55	-0.08	0.02	-0.06	0.03											
$c_{2q2l}^{[0]}$	0.0297												-0.37	0.89	-0.11	0.03	-0.21	0.04	-0.13				
$c_{2q2l}^{[1]}$	0.338												0.56	0.44	0.02		0.61	-0.10	0.34				
$c_{2q2l}^{[2]}$	0.932												0.68	0.14	0.31	-0.04	-0.52	0.13	-0.36				
$c_{2q2l}^{[3]}$	3.26												-0.25	0.04	0.78	-0.39	0.27	-0.22	-0.21				
$c_{4q}^{[0]}$	0.0568																			0.11	0.22	0.95	-0.20

- Limited information in measurements prevents constraining *all* coefficients

→ Sensitive directions in space of Wilson coefficients identified from eigenvalue decomposition of the covariance matrix

- Eigenvalues as sensitivity estimate:

$$\sigma = \frac{1}{\sqrt{\lambda}}$$

- Limits are set on linear combination of Wilson combinations in Warsaw basis
  → Transformation of basis with reduced dimensionality

Results

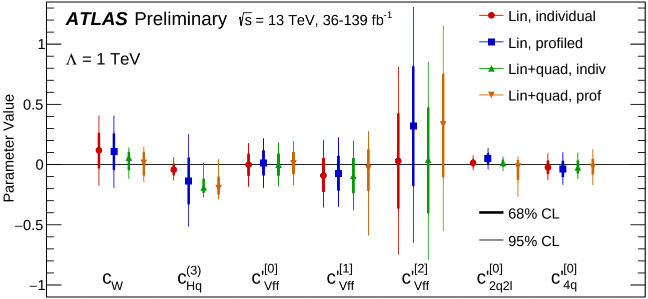

$c'^{[0]}_{Vff} \approx 0.81c_{HWB} + 0.38c_{HD} + 0.13c^{(1)}_{Hl} + 0.37c^{(3)}_{Hl} - 0.14c^{(1)}_{ll} + 0.12c^{(1)}_{Hq}$

$c'^{[1]}_{Vff} \approx 0.73c^{(1)}_{Hl} - 0.28c^{(3)}_{Hl} - 0.48c_{He} + 0.38c^{(1)}_{ll} + 0.13c^{(1)}_{Hq}$

$c'^{[2]}_{Vff} \approx 0.37c_{HWB} + 0.17c_{HD} - 0.31c^{(1)}_{Hl} - 0.53c^{(3)}_{Hl} + 0.25c_{He} + 0.59c^{(1)}_{ll} - 0.21c^{(1)}_{Hq}$

$c'^{[0]}_{2q2l} \approx -0.37c^{(1)}_{lq} + 0.89c^{(3)}_{lq} - 0.11c_{lu} - 0.21c_{eu} - 0.13c_{qe}$

$c'^{[0]}_{4q} \approx 0.11c^{(11)}_{qq} + 0.22c^{(18)}_{qq} + 0.95c^{(31)}_{qq} - 0.2c^{(38)}_{qq}$

- Limits set at 95% confidence level,
  both for the "linear" and "linear plus quadratic" models
  (difference illustrates effect of truncation of EFT expansion)
- Fits of individual coefficients, as well as combined fit

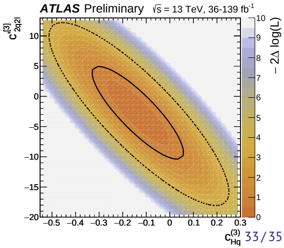

Interpretation of Quartic Electroweak Couplings

- There are no dim-6 operators that affect quartic electroweak couplings
- In VBS and triboson processes we study dim-8 operators only affecting quartic EW couplings (assuming the dim-6 coefficients are 0, and other dim-8 operators are constrained elsewhere)

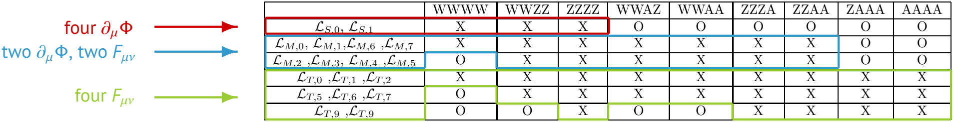

four $\partial_\mu\Phi$

two $\partial_\mu\Phi$, two $F_{\mu\nu}$

four $F_{\mu\nu}$

	WWWW	WWZZ	ZZZZ	WWAZ	WWAA	ZZZA	ZZAA	ZAAA	AAAA
$\mathcal{L}_{S,0}$, $\mathcal{L}_{S,1}$	X	X	X	O	O	O	O	O	O
$\mathcal{L}_{M,0}$, $\mathcal{L}_{M,1}$,$\mathcal{L}_{M,6}$,$\mathcal{L}_{M,7}$	X	X	X	X	X	X	X	O	O
$\mathcal{L}_{M,2}$,$\mathcal{L}_{M,3}$, $\mathcal{L}_{M,4}$,$\mathcal{L}_{M,5}$	O	X	X	X	X	X	X	O	O
$\mathcal{L}_{T,0}$,$\mathcal{L}_{T,1}$,$\mathcal{L}_{T,2}$	X	X	X	X	X	X	X	X	X
$\mathcal{L}_{T,5}$,$\mathcal{L}_{T,6}$,$\mathcal{L}_{T,7}$	O	X	X	X	X	X	X	X	X
$\mathcal{L}_{T,9}$,$\mathcal{L}_{T,9}$	O	O	X	O	O	X	X	X	X

from PRD 93, 093013 (2016)

- Literature suggests that VBS is also useful to constrain dim-6 EFT operators, see e.g. arXiv:2101.03180

⇒ Route to systematically study quartic electroweak couplings in the future

Summary

- Processes involving quartic EW couplings have become experimentally accessible
  - Observation of all major VBS processes in EW *VVjj* production in the LHC run-2
  - First observation of *pp*→*WWW* production
- Critical step in the study of EW symmetry breaking with the Higgs mechanism

- First systematic study of diboson production in SMEFT framework in ATLAS
  - Simultaneous fits of several linear combinations of Wilson coefficients
  - → Loss in stringency with improved generality

- We're well prepared to explore EW couplings in run-3 and beyond

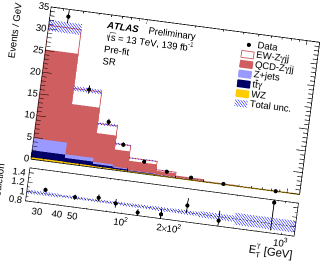

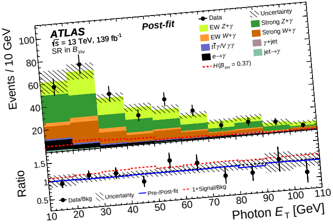

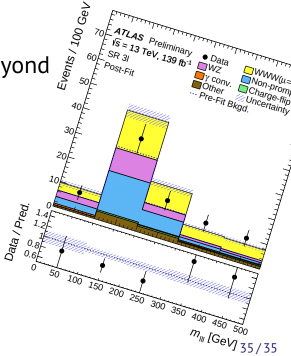

Backup

EFT Results for Additional Operators

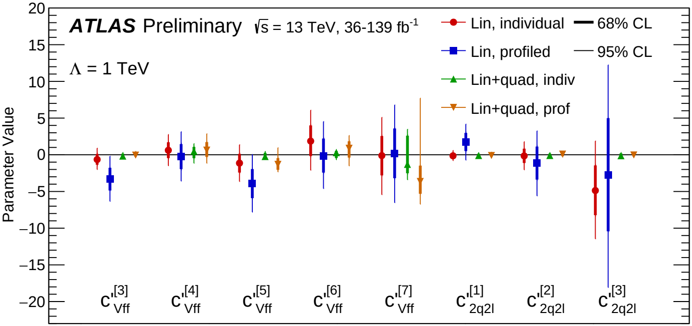

$c'^{[3]}_{Vff} \approx -0.19c^{(1)}_{Hl} - 0.14c^{(3)}_{Hl} + 0.86c^{(1)}_{Hq} + 0.41c_{Hu} - 0.17c_{Hd}$

$c'^{[4]}_{Vff} \approx -0.35c_{HWB} + 0.49c_{HD} + 0.26c^{(1)}_{Hl} + 0.35c^{(3)}_{Hl} + 0.51c_{He} + 0.38c^{(1)}_{ll} + 0.18c^{(1)}_{Hq}$

$c'^{[5]}_{Vff} \approx 0.25c_{HD} + 0.33c^{(1)}_{Hl} - 0.22c^{(3)}_{Hl} + 0.18c_{He} - 0.35c^{(1)}_{ll} - 0.3c^{(1)}_{Hq} + 0.71c_{Hu} - 0.16c_{Hd}$

$c'^{[6]}_{Vff} \approx -0.22c^{(1)}_{Hl} + 0.52c^{(3)}_{Hl} - 0.39c_{He} + 0.44c^{(1)}_{ll} - 0.22c^{(1)}_{Hq} + 0.52c_{Hu}$

$c'^{[7]}_{Vff} \approx -0.28c_{HWB} + 0.71c_{HD} - 0.31c^{(1)}_{Hl} - 0.21c^{(3)}_{Hl} - 0.5c_{He} - 0.14c^{(1)}_{ll}$

$c'^{[1]}_{2q2l} \approx 0.56c^{(1)}_{lq} + 0.44c^{(3)}_{lq} + 0.61c_{eu} - 0.1c_{ed} + 0.34c_{qe}$

$c'^{[2]}_{2q2l} \approx 0.68c^{(1)}_{lq} + 0.15c^{(3)}_{lq} + 0.33c_{lu} - 0.51c_{eu} + 0.13c_{ed} - 0.37c_{qe}$

$c'^{[3]}_{2q2l} \approx -0.27c^{(1)}_{lq} + 0.79c_{lu} - 0.39c_{ld} + 0.26c_{eu} - 0.22c_{ed} - 0.16c_{qe}$

EFT Results for Additional Operators

Wilson coefficient and operator		Final state affected at leading order			
		$e^{\pm}\nu\mu^{\mp}\nu$	$\ell^{+}\ell^{-}\ell^{\pm}\nu$	4ℓ	$\ell^{+}\ell^{-}jj$
c_G	$f^{abc}G_{\mu}^{a\nu}G_{\nu}^{b\rho}G_{\rho}^{c\mu}$				✓
c_W	$\epsilon^{IJK}W_{\mu}^{I\nu}W_{\nu}^{J\rho}W_{\rho}^{K\mu}$	✓	✓		✓
c_{HD}	$\left(H^{\dagger}D_{\mu}H\right)^{*}\left(H^{\dagger}D_{\mu}H\right)$		✓	✓	✓
c_{HWB}	$H^{\dagger}\tau^{I}H\,W_{\mu\nu}^{I}B^{\mu\nu}$	✓	✓	✓	✓
$c_{Hl}^{(1)}$	$(H^{\dagger}i\overleftrightarrow{D}_{\mu}H)(\bar{l}\gamma^{\mu}l)$	✓	✓	✓	✓
$c_{Hl}^{(3)}$	$(H^{\dagger}i\overleftrightarrow{D}_{\mu}^{I}H)(\bar{l}\tau^{I}\gamma^{\mu}l)$	✓	✓	✓	✓
c_{He}	$(H^{\dagger}i\overleftrightarrow{D}_{\mu}H)(\bar{e}\gamma^{\mu}e)$		✓	✓	✓
$c_{Hq}^{(1)}$	$(H^{\dagger}i\overleftrightarrow{D}_{\mu}H)(\bar{q}\gamma^{\mu}q)$	✓	✓	✓	✓
$c_{Hq}^{(3)}$	$(H^{\dagger}i\overleftrightarrow{D}_{\mu}^{I}H)(\bar{q}\tau^{I}\gamma^{\mu}q)$	✓	✓	✓	✓
c_{Hu}	$(H^{\dagger}i\overleftrightarrow{D}_{\mu}H)(\bar{u}\gamma^{\mu}u)$	✓	✓	✓	✓
c_{Hd}	$(H^{\dagger}i\overleftrightarrow{D}_{\mu}H)(\bar{d}\gamma^{\mu}d)$	✓	✓	✓	✓
$c_{ll}^{(1)}$	$(\bar{l}\gamma_{\mu}l)(\bar{l}\gamma^{\mu}l)$	✓	✓	✓	✓
$c_{lq}^{(1)}$	$(\bar{l}\gamma_{\mu}l)(\bar{q}\gamma^{\mu}q)$	✓	✓	✓	(✓)
$c_{lq}^{(3)}$	$(\bar{l}\gamma_{\mu}\tau^{I}l)(\bar{q}\gamma^{\mu}\tau^{I}q)$	✓	✓	✓	(✓)
c_{eu}	$(\bar{e}\gamma_{\mu}e)(\bar{u}\gamma^{\mu}u)$			✓	(✓)
c_{ed}	$(\bar{e}\gamma_{\mu}e)(\bar{d}\gamma^{\mu}d)$			✓	(✓)
c_{ed}	$(\bar{e}\gamma_{\mu}e)(\bar{d}\gamma^{\mu}d)$			✓	(✓)
c_{lu}	$(\bar{l}\gamma_{\mu}l)(\bar{u}\gamma^{\mu}u)$	✓		✓	(✓)
c_{ld}	$(\bar{l}\gamma_{\mu}l)(\bar{d}\gamma^{\mu}d)$	✓		✓	(✓)
c_{qe}	$(\bar{q}\gamma_{\mu}q)(\bar{e}\gamma^{\mu}e)$		✓	✓	(✓)
$c_{qq}^{(1,1)}$	$(\bar{q}\gamma_{\mu}q)(\bar{q}\gamma^{\mu}q)$				✓
$c_{qq}^{(1,8)}$	$(\bar{q}T^{a}\gamma_{\mu}q)(\bar{q}T^{a}\gamma^{\mu}q)$				✓
$c_{qq}^{(3,1)}$	$(\bar{q}\sigma^{i}\gamma_{\mu}q)(\bar{q}\sigma^{i}\gamma^{\mu}q)$				✓
$c_{qq}^{(3,8)}$	$(\bar{q}\sigma^{i}T^{a}\gamma_{\mu}q)(\bar{q}\sigma^{i}T^{a}\gamma^{\mu}q)$				✓
$c_{uu}^{(1)}$	$(\bar{u}\gamma_{\mu}u)(\bar{u}\gamma^{\mu}u)$				✓
$c_{uu}^{(8)}$	$(\bar{u}T^{a}\gamma_{\mu}u)(\bar{u}T^{a}\gamma^{\mu}u)$				✓
$c_{dd}^{(1)}$	$(\bar{d}\gamma_{\mu}d)(\bar{d}\gamma^{\mu}d)$				✓
$c_{dd}^{(8)}$	$(\bar{d}T^{a}\gamma_{\mu}d)(\bar{d}T^{a}\gamma^{\mu}d)$				✓
$c_{ud}^{(1)}$	$(\bar{u}\gamma_{\mu}u)(\bar{d}\gamma^{\mu}d)$				✓
$c_{ud}^{(8)}$	$(\bar{u}T^{a}\gamma_{\mu}u)(\bar{d}T^{a}\gamma^{\mu}d)$				✓
$c_{qu}^{(1)}$	$(\bar{q}\gamma_{\mu}q)(\bar{u}\gamma^{\mu}u)$				✓
$c_{qu}^{(8)}$	$(\bar{q}T^{a}\gamma_{\mu}q)(\bar{u}T^{a}\gamma^{\mu}u)$				✓
$c_{qd}^{(1)}$	$(\bar{q}\gamma_{\mu}q)(\bar{d}\gamma^{\mu}d)$				✓
$c_{qd}^{(8)}$	$(\bar{q}T^{a}\gamma_{\mu}q)(\bar{d}T^{a}\gamma^{\mu}d)$				✓

Eigenvalue Decomposition – Full Covariance Matrix

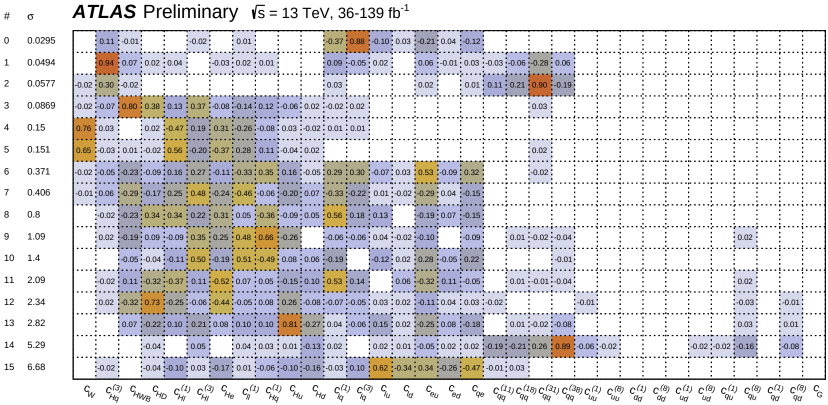

ATLAS **Preliminary** $\sqrt{s}$ = 13 TeV, 36-139 fb^{-1}

#	σ	c_W	$c_{Hq}^{(3)}$	c_{HWB}	c_{HD}	$c_{Hl}^{(1)}$	$c_{Hl}^{(3)}$	c_{He}	$c_{ll}^{(1)}$	$c_{Hq}^{(1)}$	c_{Hu}	c_{Hd}	$c_{lq}^{(1)}$	$c_{lq}^{(3)}$	c_{lu}	c_{ld}	c_{eu}	c_{ed}	c_{qe}	$c_{qq}^{(11)}$	$c_{qq}^{(18)}$	$c_{qq}^{(31)}$	$c_{qq}^{(38)}$	$c_{uu}^{(1)}$	$c_{uu}^{(8)}$	$c_{dd}^{(1)}$	$c_{dd}^{(8)}$	$c_{ud}^{(1)}$	$c_{ud}^{(8)}$	$c_{qu}^{(1)}$	$c_{qu}^{(8)}$	$c_{qd}^{(1)}$	$c_{qd}^{(8)}$	c_G
0	0.0295		0.11	-0.01			-0.02		0.01				-0.37	0.88	-0.10	0.03	-0.21	0.04	-0.12															
1	0.0494		0.94	0.07	0.02	0.04		-0.03	0.02	0.01			0.09	-0.05	0.02		0.06	-0.01	0.03	-0.03	-0.06	-0.28	0.06											
2	0.0577	-0.02	0.30	-0.02									0.03				0.02		0.01	0.11	0.21	0.90	-0.19											
3	0.0869	-0.02	-0.07	0.80	0.38	0.13	0.37	-0.08	-0.14	0.12	-0.06	0.02	-0.02	0.02								0.03												
4	0.15	0.76	0.03		0.02	-0.47	0.19	0.31	-0.26	-0.08	0.03	-0.02	0.01	0.01																				
5	0.151	0.65	-0.03	0.01	-0.02	0.56	-0.20	-0.37	0.28	0.11	-0.04	0.02										0.02												
6	0.371	-0.02	-0.05	-0.23	-0.09	0.16	0.27	-0.11	-0.33	0.35	0.16	-0.05	0.29	0.30	-0.07	0.03	0.53	-0.09	0.32			-0.02												
7	0.406	-0.01	0.06	-0.29	-0.17	0.25	0.48	-0.24	-0.46	-0.06	-0.20	0.07	-0.33	-0.22	0.01	-0.02	-0.29	0.04	-0.15															
8	0.8		-0.02	-0.23	0.34	0.34	0.22	0.31	0.05	-0.36	-0.09	0.05	0.56	0.18	0.13		-0.19	0.07	-0.15															
9	1.09		0.02	-0.19	0.09	-0.09	0.35	0.25	0.48	0.66	-0.26		-0.06	-0.06	0.04	-0.02	-0.10		-0.09		0.01	-0.02	-0.04								0.02			
10	1.4			-0.05	-0.04	-0.11	0.50	-0.19	0.51	-0.49	0.08	0.06	-0.19		-0.12	0.02	0.28	-0.05	0.22				-0.01											
11	2.09		-0.02	0.11	-0.32	-0.37	0.11	-0.52	0.07	0.05	-0.15	0.10	0.53	0.14		0.06	-0.32	0.11	-0.05		0.01	-0.01	-0.04								0.02			
12	2.34		0.02	-0.32	0.73	-0.25	-0.06	-0.44	-0.05	0.08	0.26	-0.08	-0.07	-0.05	0.03	0.02	-0.11	0.04	0.03	-0.02				-0.01							-0.03		-0.01	
13	2.82			0.07	-0.22	0.10	0.21	0.08	0.10	0.10	0.81	-0.27	0.04	-0.06	0.15	0.02	-0.25	0.08	-0.18		0.01	-0.02	-0.08								0.03		0.01	
14	5.29				-0.04		0.05		0.04	0.03	0.01	-0.13	0.02		0.02	0.01	-0.05	0.02	0.02	-0.19	-0.21	0.26	0.89	-0.06	-0.02				-0.02	-0.02	-0.16		-0.08	
15	6.68		-0.02		-0.04	-0.10	0.03	-0.17	0.01	-0.06	-0.10	-0.16	-0.03	0.10	0.62	-0.34	0.34	-0.26	-0.47	-0.01	0.03													

Correlations Final Fit

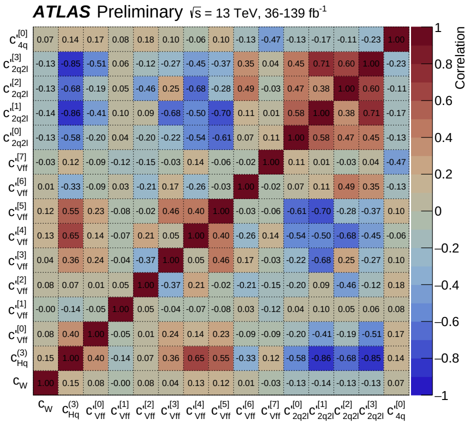

ATLAS Preliminary $\sqrt{s}$ = 13 TeV, 36-139 fb^{-1}

	c_W	$c^{(3)}_{Hq}$	$c'^{[0]}_{Vff}$	$c'^{[1]}_{Vff}$	$c'^{[2]}_{Vff}$	$c'^{[3]}_{Vff}$	$c'^{[4]}_{Vff}$	$c'^{[5]}_{Vff}$	$c'^{[6]}_{Vff}$	$c'^{[7]}_{Vff}$	$c'^{[0]}_{2q2l}$	$c'^{[1]}_{2q2l}$	$c'^{[2]}_{2q2l}$	$c'^{[3]}_{2q2l}$	$c'^{[0]}_{4q}$
$c'^{[0]}_{4q}$	0.07	0.14	0.17	0.08	0.18	0.10	-0.06	0.10	-0.13	-0.47	-0.13	-0.17	-0.11	-0.23	1.00
$c'^{[3]}_{2q2l}$	-0.13	-0.85	-0.51	0.06	-0.12	-0.27	-0.45	-0.37	0.35	0.04	0.45	0.71	0.60	1.00	-0.23
$c'^{[2]}_{2q2l}$	-0.13	-0.68	-0.19	0.05	-0.46	0.25	-0.68	-0.28	0.49	-0.03	0.47	0.38	1.00	0.60	-0.11
$c'^{[1]}_{2q2l}$	-0.14	-0.86	-0.41	0.10	0.09	-0.68	-0.50	-0.70	0.11	0.01	0.58	1.00	0.38	0.71	-0.17
$c'^{[0]}_{2q2l}$	-0.13	-0.58	-0.20	0.04	-0.20	-0.22	-0.54	-0.61	0.07	0.11	1.00	0.58	0.47	0.45	-0.13
$c'^{[7]}_{Vff}$	-0.03	0.12	-0.09	-0.12	-0.15	-0.03	0.14	-0.06	-0.02	1.00	0.11	0.01	-0.03	0.04	-0.47
$c'^{[6]}_{Vff}$	0.01	-0.33	-0.09	0.03	-0.21	0.17	-0.26	-0.03	1.00	-0.02	0.07	0.11	0.49	0.35	-0.13
$c'^{[5]}_{Vff}$	0.12	0.55	0.23	-0.08	-0.02	0.46	0.40	1.00	-0.03	-0.06	-0.61	-0.70	-0.28	-0.37	0.10
$c'^{[4]}_{Vff}$	0.13	0.65	0.14	-0.07	0.21	0.05	1.00	0.40	-0.26	0.14	-0.54	-0.50	-0.68	-0.45	-0.06
$c'^{[3]}_{Vff}$	0.04	0.36	0.24	-0.04	-0.37	1.00	0.05	0.46	0.17	-0.03	-0.22	-0.68	0.25	-0.27	0.10
$c'^{[2]}_{Vff}$	0.08	0.07	0.01	0.05	1.00	-0.37	0.21	-0.02	-0.21	-0.15	-0.20	0.09	-0.46	-0.12	0.18
$c'^{[1]}_{Vff}$	-0.00	-0.14	-0.05	1.00	0.05	-0.04	-0.07	-0.08	0.03	-0.12	0.04	0.10	0.05	0.06	0.08
$c'^{[0]}_{Vff}$	0.08	0.40	1.00	-0.05	0.01	0.24	0.14	0.23	-0.09	-0.09	-0.20	-0.41	-0.19	-0.51	0.17
$c^{(3)}_{Hq}$	0.15	1.00	0.40	-0.14	0.07	0.36	0.65	0.55	-0.33	0.12	-0.58	-0.86	-0.68	-0.85	0.14
c_W	1.00	0.15	0.08	-0.00	0.08	0.04	0.13	0.12	0.01	-0.03	-0.13	-0.14	-0.13	-0.13	0.07

Couplings in *VVjj* production

$$\begin{tikzcd}
\textbf{LO} & & \mathcal{O}\left(\alpha^6\right) \arrow[dl, "\mathrm{EW}"'] \arrow[dr, "\mathrm{QCD}"'] & & \mathcal{O}\left(\alpha_\mathrm{s}\alpha^5\right) \arrow[dl, "\mathrm{EW}"'] \arrow[dr, "\mathrm{QCD}"'] & & \mathcal{O}\left(\alpha_\mathrm{s}^2\alpha^4\right) \arrow[dl, "\mathrm{EW}"'] \arrow[dr, "\mathrm{QCD}"'] & \\
\textbf{NLO} & \mathcal{O}\left(\alpha^7\right) & & \mathcal{O}\left(\alpha_\mathrm{s}\alpha^6\right) & & \mathcal{O}\left(\alpha_\mathrm{s}^2\alpha^5\right) & & \mathcal{O}\left(\alpha_\mathrm{s}^3\alpha^4\right)
\end{tikzcd}$$

WH Measurements

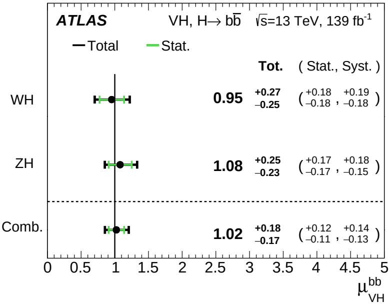

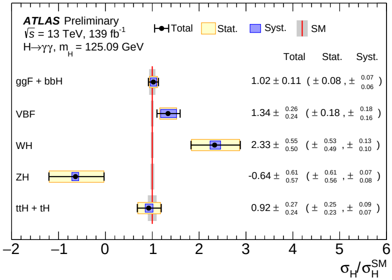

- Measurement of *VH*, $H \to b\bar{b}$ in 139 fb^{-1}
- EPJC 81 (2021) 178

- Measurement of *VH*, $H \to \gamma\gamma$ in 139 fb^{-1}
- ATLAS-CONF-2020-026
- Large negative correlation (–42%) between *WH* and *ZH*

$\sum$: $\sigma\mathcal{B}/(\sigma\mathcal{B})_{\text{SM}} = (5.9\pm1.4\,\text{fb})/(4.53\pm0.12\,\text{fb})$, *p*-value= 50%

WWW in CMS

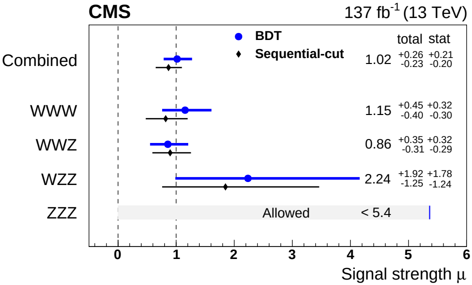

Process	Cross section (fb)
Treating Higgs boson contributions as signal	
VVV	$1010^{+210}_{-200}{}^{+150}_{-120}$
WWW	$590^{+160}_{-150}{}^{+160}_{-130}$
WWZ	$300^{+120}_{-100}{}^{+50}_{-40}$
WZZ	$200^{+160}_{-110}{}^{+70}_{-20}$
ZZZ	<200
Treating Higgs boson contributions as background	
VVV	$370^{+140}_{-130}{}^{+80}_{-60}$
WWW	$190^{+110}_{-100}{}^{+80}_{-70}$
WWZ	$100\,^{+80}_{-70}{}^{+30}_{-30}$
WZZ	$110^{+100}_{-70}{}^{+30}_{-10}$
ZZZ	<80

(Measured cross sections)

From Phys. Rev. Lett. 125 (2020) 151802

VVV in ATLAS

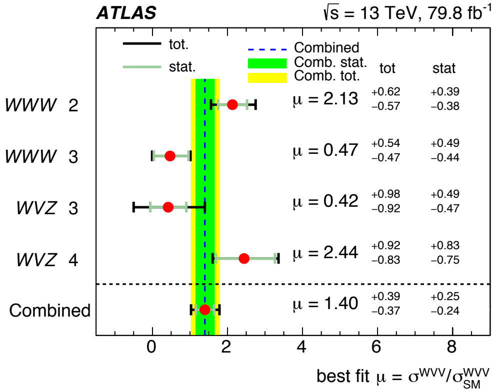

From Phys. Lett. B 798 (2019) 134913

WWW Event Yields

	$e^\pm e^\pm$	$e^\pm\mu^\pm$	$\mu^\pm\mu^\pm$	3ℓ
WWW	29.3 ± 4.4	128 ± 19	84 ± 12	35.8 ± 5.2
WZ	80.6 ± 5.7	344 ± 22	171 ± 10	16.4 ± 1.4
Charge-flip	30.3 ± 7.2	18.8 ± 4.5	–	1.7 ± 0.4
γ conversions	62.1 ± 8.7	142 ± 15	–	1.5 ± 0.1
Non-prompt	16.6 ± 4.1	138 ± 24	98 ± 21	26.3 ± 2.9
Other	22.8 ± 3.7	102 ± 15	59.7 ± 9.0	8.0 ± 0.9
Total predicted	242 ± 11	872 ± 22	414 ± 17	89.7 ± 5.4
Data	242	885	418	79

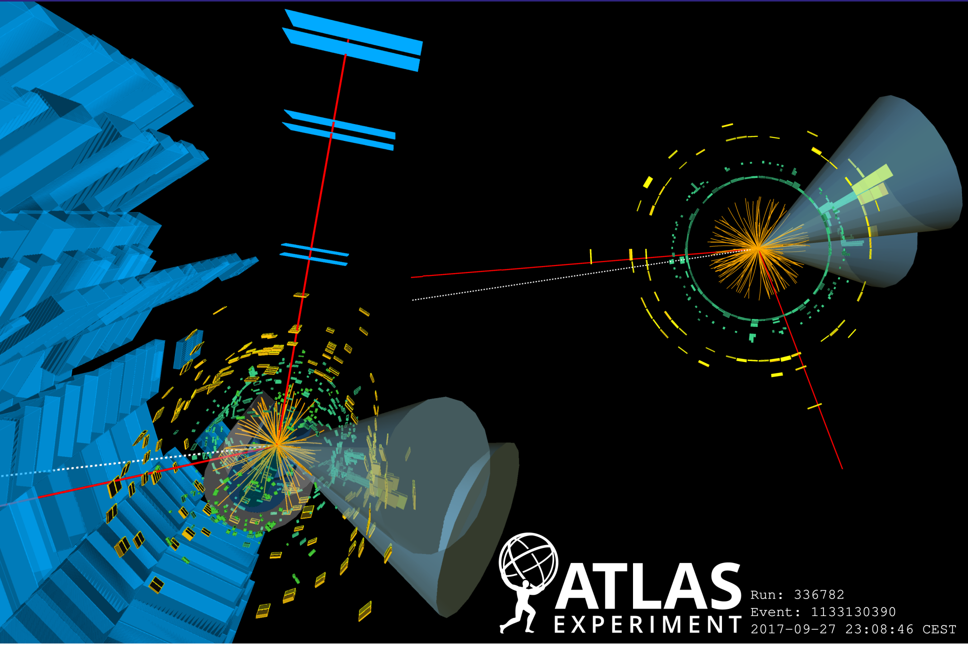

$WWW\rightarrow\mu^{+}\nu\mu^{+}\nu jj$ candidate event. The jets have $p_{\mathrm{T}}=186$ GeV and $p_{\mathrm{T}}=84$ GeV, with $m_{jj}=80.9$ GeV. The BDT score is 0.86.

$Z(\rightarrow\nu\nu)\gamma$ Selection

Variable	SR	$W^{\gamma}_{\mu\nu}$ CR	$W^{\gamma}_{e\nu}$ CR	$Z^{\gamma}_{\text{Rev.Cen.}}$ CR	Fake-e CR	Low-$E_{\text{T}}^{\text{miss}}$ VR
$p_{\text{T}}(j_1)$ [GeV]	> 60					
$p_{\text{T}}(j_2)$ [GeV]	> 50					
$p_{\text{T}}(j_{>2})$ [GeV]	> 25					
N_{jet}	2,3					
$N_{b\text{-jet}}$	< 2					
$\Delta\phi_{\text{jj}}$	< 2.5 [2.0]					
$\lvert\Delta\eta_{\text{jj}}\rvert$	> 3.0					
$\eta(j_1) \times \eta(j_2)$	< 0					
C_3	< 0.7					
m_{jj} [TeV]	> 0.25					0.25–1.0
$E_{\text{T}}^{\text{miss}}$ [GeV]	> 150	–	> 80	> 150	< 80	110–150
$E_{\text{T}}^{\text{miss,lep-rm}}$ [GeV]	–	> 150	> 150	–	> 150	110–150
$E_{\text{T}}^{\text{jets,no-jvt}}$ [GeV]	> 130					> 100
$\Delta\phi(j_i, \vec{E}_{\text{T}}^{\text{miss,lep-rm}})$	> 1.0					
N_{γ}	1					
$p_{\text{T}}(\gamma)$ [GeV]	$> 15, < 110$ [$> 15, < \max(110, 0.733 \times m_{\text{T}})$]					
C_{γ}	> 0.4	> 0.4	> 0.4	< 0.4	> 0.4	> 0.4
$\Delta\phi(\gamma, \vec{E}_{\text{T}}^{\text{miss,lep-rm}})$	> 1.8 [–]					
N_{ℓ}	0	1 μ	1 e	0	1 e	0
$p_{\text{T}}(\ell)$ [GeV]	–	> 30	> 30	–	> 30	–

$Z(\to\nu\nu)\gamma$ Uncertainties

Source	1σ Uncertainty on $\mu_{Z\gamma_{\mathrm{EW}}}$	1σ Uncertainty on $\mathcal{B}_{\mathrm{inv}}$	1σ Uncertainty on $\mathcal{B}(H\to\gamma\gamma_{\mathrm{d}})$
Jet scale and resolution	0.076	0.045	0.0011
$V\gamma+$jets theory	0.067	0.044	0.0018
pile-up	0.040	0.021	0.0004
Photon	0.035	0.031	0.0011
$e\to\gamma$, jet$\to e,\gamma$ Bkg.	0.035	0.034	0.0028
Lepton	0.027	0.003	0.0008
$E_{\mathrm{T}}^{\mathrm{miss}}$	0.023	0.018	0.0003
Signal theory shape	0.020	–	–
Signal theory acceptance	0.12	–	–
Data stats.	0.16	0.11	0.0056
$W\gamma+$jets/$Z\gamma+$jets Norm.	0.073	0.013	0.0004
MC stats.	0.063	0.046	0.0026
Total	0.25	0.15	0.0073

$Z(\rightarrow \nu\nu)\gamma$ Event Yields

Process	Fake-e CR	$W^{\gamma}_{e\nu}$ CR	$W^{\gamma}_{\mu\nu}$ CR	$Z^{\gamma}_{\text{Rev.Cen.}}$ CR	SR - m_{jj} [TeV]			
					0.25-0.5	0.5-1.0	1.0-1.5	≥ 1.5
Strong $Z\gamma+$jets	8 ± 8	0 ± 1	3 ± 2	50 ± 12	20 ± 6	54 ± 12	13 ± 5	5 ± 2
EW $Z\gamma+$jets	0.6 ± 0.2	0.3 ± 0.2	0.4 ± 0.2	7 ± 2	4 ± 1	30 ± 7	25 ± 5	36 ± 7
Strong $W\gamma+$jets	43 ± 9	47 ± 9	133 ± 21	24 ± 6	22 ± 6	35 ± 10	9 ± 3	3 ± 1
EW $W\gamma+$jets	19 ± 6	31 ± 7	59 ± 13	1.4 ± 0.5	2 ± 1	6 ± 1	4 ± 1	5 ± 1
jet$\rightarrow\gamma$	1 ± 1	2 ± 2	3 ± 2	2 ± 2	1 ± 1	2 ± 2	1 ± 1	0.4 ± 0.3
jet$\rightarrow e$	34 ± 17	5 ± 3	–	–	–	–	–	–
$e\rightarrow\gamma$	–	2.7 ± 0.4	2.9 ± 0.4	13 ± 1	6 ± 1	11 ± 1	2.6 ± 0.4	1.4 ± 0.3
$\gamma+$jet	–	–	–	0.7 ± 0.5	0.7 ± 0.5	0.4 ± 0.3	0.1 ± 0.1	0.1 ± 0.1
$t\bar{t}\gamma/V\gamma\gamma$	3 ± 1	9 ± 2	13 ± 2	3 ± 1	2 ± 1	4 ± 1	0.4 ± 0.2	0.1 ± 0.1
Fitted Yields	108 ± 10	96 ± 8	213 ± 14	102 ± 9	58 ± 6	143 ± 12	54 ± 5	52 ± 6
Data	108	95	216	100	52	153	50	52
Data/Fit	1.00 ± 0.14	0.99 ± 0.12	1.01 ± 0.09	0.98 ± 0.13	0.90 ± 0.15	1.07 ± 0.11	0.93 ± 0.16	0.99 ± 0.18

$Z(\rightarrow\ell\ell)\gamma$ Event Yields